Comparison of Three Ways to Assess the Influence Range of Different Artificial Reefs

Huang Luiyi, Cheng Hui, Tang Yanli, Yang Qian, and Wang Xinxin

***Abstract*—Artificial reefs have been constructed throughout the world, but there is no uniform method to assess the influence range of artificial reef. The physical influence on surrounding flow of artificial reef can be mainly represented by three kinds of flow pattern including upwelling current, wake flow and back eddy. In this paper we compare three different methods, based on influence length, influence area, and influence volume, to find out an effective method to indicate the impact effect of the artificial reef. The numerical method of renormalization group *k-ε* turbulence model is used to calculate the characteristics of the flow field around four kinds of artificial reefs and the above three kinds of assessment methods are applied to compare the flow field. The results show that: 1. The influence volume is better than the other two in general; 2. Influence area and length can be a misjudgment sometimes especially when the artificial reef is asymmetric; 3. Influence area is a better way to show the diversity of wake flow; 4. Influence length cannot reflect the back eddy. It is recommended to use the influence volume as the main measurement assessing the influence range of artificial reef. Meanwhile, the influence area may be a good indicator to assess the wake flow and the influence length just be a simple comparison.**

***Index Terms*—Numerical simulation, assess method, influence length, influence area, influence volume.**

I. Introduction

The artificial reef is an important submerged structure used to optimize marine ecological environments and to improve the fisheries resources. With various of designs and structures, an artificial reef reshapes the local flow field through generating upwelling flow, decelerating flow, and back eddy. The change of flow can bring nutrient-exchange in the water and the local primary productivity enhancing. Many maritime countries established organizations and invested in the scientific research of artificial reef, because of its ability to increase the efficiency of fishery resource harvest [1]. The artificial reefs placed on the seafloor create new habitats for the marine flora and fauna. Different kinds of fish have different reactions to the surrounding environment and preference to the flow characters [2]. Since the structure and shape of the artificial reef can be various, the flow fields around it could be complex and changeable [3]. The current changes not only provide flow variations but also facilitate nutrient transport.

The research methods on the physical influence of artificial reef include theoretical analysis, flume test, wind tunnel experiments, particle image velocity (PIV) experiments, and computational fluid dynamics (CFD). With the development of CFD theories and high-performance computer, the precision and accuracy of simulation have been largely promoted. The numerical simulation results have been verified by flume test and PIV experiment according to Zheng's result [4]. A number of researchers suggest that the CFD could be applied to the prediction of forces, stress, deformation, and flow fields of or around the artificial reef.

There are researchers using CFD to investigate the influence on the flow field around the artificial reefs. Kim and Lui used the wake flow length and influence area to investigate the influence effect of different kinds of artificial reefs [5], [6]. Jiang used the upwelling heights and back eddy areas to study the influence effect of artificial reef [7], [8]. Generally, the methods of evaluating the influence from artificial reefs can be classified by different dimensions into three aspects, namely influence length, influence area, and influence volume, which represents one-dimensional, two-dimensional, and three-dimensional, respectively. In this paper, authors compare the above three methods on four different artificial reef models through CFD to find out which method is more suitable and representative for assess the physical influence effect of the artificial reefs.

II. Theoretical Background

A. Governing Equations

Regarding the numerical calculations for the artificial reefs with complex structure, this study uses Reynolds-averaged Navier-Strokes (RANS) equations to calculate the flow field. The continuity equation (Eq.1) and momentum equations (Eq.2) in the RANS equation can be written in Cartesian tensor form as:

$$\frac{\partial \rho}{\partial t}+\frac{\partial}{\partial x_i}\left(\rho u_i\right)=0 \tag{1}$$

$$\frac{\partial}{\partial t}\left(\rho u_i\right)+\frac{\partial}{\partial x_j}\left(\rho u_i u_j\right)=-\frac{\partial p}{\partial x_i}+\frac{\partial}{\partial x_j}\cdot \left(\mu\left(\frac{\partial u_i}{\partial x_j}+\frac{\partial u_j}{\partial x_i}-\frac{2}{3}\delta_{ij}\frac{\partial u_l}{\partial x_l}\right)\right)+\frac{\partial}{\partial x_j}\left(-\rho\overline{u_i^{'}u_j^{'}}\right) \tag{2}$$

Manusript received December 28, 2015; revised February 28, 2016.

Huang Luiyi, Cheng Hui, Tang Yanli, and Wang Xinxin are with the Ocean University of China, Qingdao, 266003, China (e-mail: huangly@ouc.edu.cn, chenghui.qd@live.cn, tangyanli@ouc.edu.cn, wxinxin@ouc.edu.cn).

Yang Qian is with the Tokyo University of Marine Science and Technology, 108-0075, Japan (e-mail: yangqian9202@gmail.com).

DOI: 10.7763/IJET.2017.V9.953

where u_i and u'_i are the mean and fluctuating velocity components (i= 1, 2, 3), p represents the pressure and $-\rho\overline{u_i'u_j'}$ is the Reynolds stress. The additional terms compared to Navier-Strokes equation represent the effects of turbulence. This study uses the Renormalization group k-ε Model from Fluent 15.0 code to calculate the flow field. This model uses the finite volume method as the numerical method to calculate the discretized RANS equation, which increases both the accuracy and computational efficiency of computer programs. In this study, the following hypotheses are used to simplify the calculation:

1) The fluid is incompressible, viscous and Newtonian fluid;
2) The flow is isothermal and negligible the heat exchange;
3) The velocity of flow is in a steady state;
4) The roughness of artificial reef surface can be neglected.

B. Technical Terms

In this paper, the vertical plane and horizontal plane are regarded as the typical reference plane, defined in Fig. 1. The vertical plane is a vertical section of y=0 m (known as the xoz plane). The horizontal plane is a horizontal section of z=1/2 reef height. At the same time, the two lines (vertical reference line and horizontal reference line) cross the geometric center in the reference planes, respectively. The influence lengths of the four artificial reef are calculated based on the two lines as above. The influence area is calculated by domain integral computation on the two typical reference planes as above. The influence volumes are calculated from an integral program which is written using Matlab.

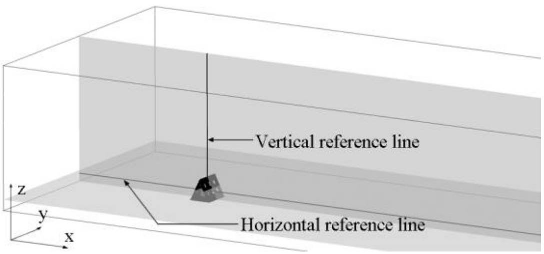

Fig. 1. The position of the vertical plane, horizontal plane, vertical reference line, and the horizontal reference line.

Several technical terms are introduced here for the later comparisons. The upwelling flow is defined as the domain where the z-component velocity is equal or greater than ten percent of the inlet flow velocity. The wake flow is defined as the domain where the velocity is smaller than 0.8 times the inlet velocity. A clockwise rotation eddy appears at the back of the artificial reef, known as the back eddy flow, according to Liu. But due to the length and area of back eddy are difficult to quantitative analysis, it is just compared the volume of the back eddy in section four.

III. Materials and Methods

Fig. 2 shows the geometry parameters and case number of the artificial reef. Case 1 is a triangular prism shell with 6 holes on its two slope walls. Case 2 is a hemispherical shell with 5 holes on its surface. Case 3 and Case 4 are both based on a cube shell but have a difference on their top structure. All the cases have the same height. The detail information of the geometry of the four cases is presented in Table I and Fig. 2.

TABLE I: Dimensions of Artificial Reefs

Case number	Height (m)	Length (m)	Width (m)	Physical volume ($\times10^{-6}$m^3)
Case 1	0.15	0.15	0.15	1687.50
Case 2	0.15	0.30	0.30	7068.58
Case 3	0.15	0.15	0.15	3375.00
Case 4	0.15	0.15	0.15	3375.00

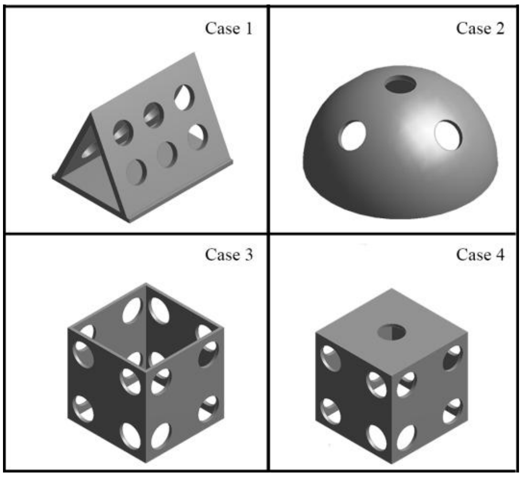

Fig. 2. The four representative general artificial reefs.

The fluid is assumed to be incompressible. The velocity at the inlet boundary is assumed to be a uniform flow in the x-direction while the relative pressure is set to 0 Pa at the outlet boundary. The inlet flow velocity is set as a constant value, 0.2 m/s, in all the four cases, which is suitable and independent of wake characteristics according to D. Kim's results [5]. The turbulence is set to 5% and the surface of the artificial reef is assumed to be a smooth and non-slip wall. The bottom boundary is set as a rough wall to simulate the seafloor. The other boundaries are slip wall without any shear force and relative velocity of inflow to eliminate the wall effects [9]. In accordance with the dimension of the reef block, the computational domain is 6 m long, 1 m wide, and 1 m deep. The bottom center of the reef block is set as the coordination origin, which is 1 m downstream from the inlet boundary. The details of the computing domain are presented in the Fig. 3.

The total number of nodes and elements are approximately 1.45×10^6 and 8.47×10^6 respectively. A series of meshing tests are performed to determining the optimal mesh type, grid size, and growth ratio. The near-wall region matches the height of the first cell near the artificial reef surface with Δy = 0.01 mm. The tetrahedral mesh accounts for a large number of the meshes for the complex geometric features of the artificial reef. The maximum size of the mesh is 0.05 m.

In the numerical analysis, the calculation is carried out by ANSYS Workbench and Fluent 15.0. The renormalization group k-ε turbulent model is chosen as the turbulence model for its good performance for the accuracy and speed [10]-[12]. The SIMPLIC algorithm is used for pressure-velocity coupling [13]. The residual of continuity and velocity is set as 1×10^{-4}.

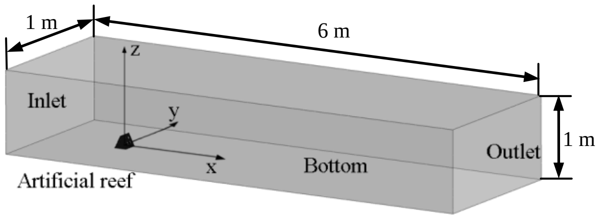

Fig. 3. Calculation domain and boundary conditions.

IV. Result and Discussion

A. Influence Length

Fig. 4 shows the current velocity on the horizontal reference line. Here the velocity refers to the component of x-direction to indicate the velocity changes more clearly. The x-component of velocity rapidly changes in front of an artificial reef and becomes stable after a certain distance from the back of artificial reef. The velocity of wake flow is a little smaller than the inlet current in all the four cases. The wake flow length is defined as the distance between the back face of artificial reefs and the point where the velocity value equal 0.16 m/s (80% of inlet velocity) [6], which means the influence from artificial reef becomes limited after that point. The wake flow length of the four cases shows no obvious differences from Fig. 4. But when using the relative wake length which is calculated by dividing the original wake flow length by the length of the artificial reef, the difference can be easily detected (Fig. 6). Case 3 and Case 4 have a similar wake flow pattern because of their similar geometry. Also, they have a longer wake flow length compared with Case 1 and Case 2, which illustrates that the cube shell has a larger influence effect on flow direction.

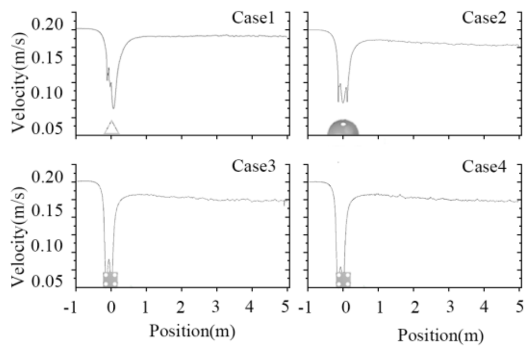

Fig. 4. Distribution of flow velocities along the horizontal reference line.

Fig. 5 shows the current velocity on the vertical reference line. Here the velocity refers to the component of z-direction to indicate the velocity changes in the vertical line more clearly. The z-component of velocity rapidly changes around the artificial reef and tends to zero at a certain distance above the top of the artificial reef. The upwelling flow length is defined as the distance between the top of artificial reefs and the point where the z-component of velocity value equal 0.02 m/s (10% of inlet velocity) [14]. In the Fig. 6, the relative length for the upwelling flow is calculated by dividing the original upwelling flow length by the height of the artificial reef. The result shows that the triangular prism shell has the longest upwelling flow length. This can be explained from Fig. 7 in the next part that the slope plane has a directed effect on the flow. The other three cases have the similar upwelling flow length. One thing should be noticed that Case 3 has a clear downwelling flow on the vertical reference line in Fig. 5. It can be inferred that the cover cap can resist the downwelling flow. In general, the Case 2 has the smallest influence effect compared with others and the cube shells have a longer wake flow length, while the triangular prism shell has a longer upwelling flow length.

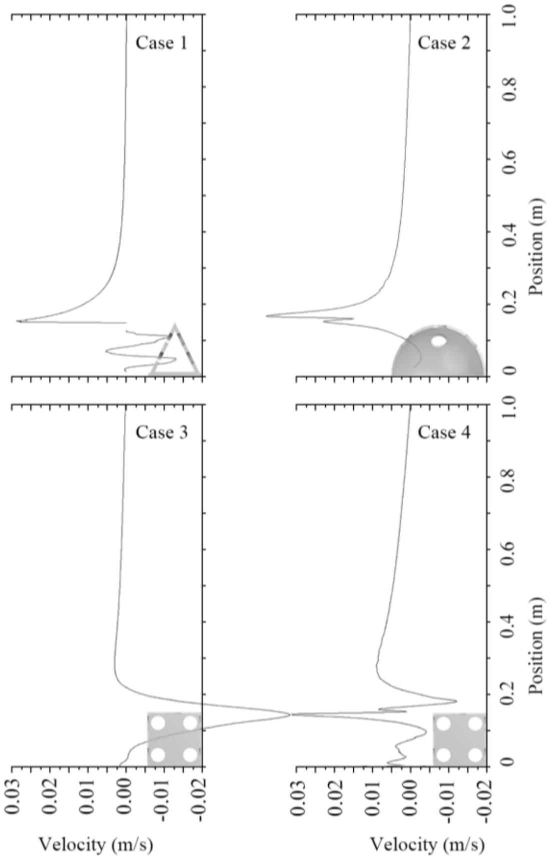

Fig. 5. Distribution of flow velocities along the vertical reference line.

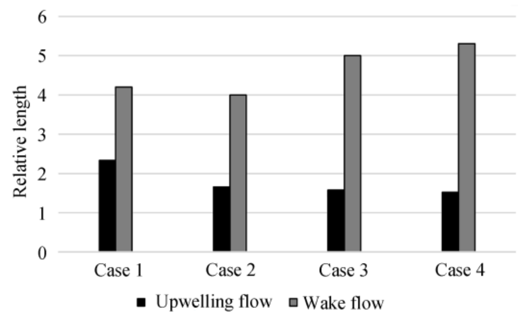

Fig. 6. Relative influence length of the four cases.

B. Influence Area

Fig. 7 and Fig. 8 show the velocity distribution in the vertical plane and horizontal plane of the four cases. The velocity value in the figures is represented by colors, which can be read from the color bar on the lower left corner. The curve lines with the black arrows represent the streamlines and velocity vector. The geometrical centers of the four cases are put in a certain line to compare the influence area more conveniently. From the Fig. 7, it can be observed that Case 1 has the largest influence area and the Case 3 and Case 4 have the smallest influence area. Case 1 has a clear and large back eddy comparing with others, which cannot be deduced from the length analysis. All the four cases have a complex flow-decelerating region inside the artificial reef. There are flow-accelerating regions at the upfront of the artificial reef and flow-decelerating regions at front and back of the artificial reef in all the four cases. Compared with Case 3 and Case 4, the cube shell with a cover cap (Case 4) have a larger upwelling flow area. The influence areas of the four cases on this plane are presented in Fig. 9.

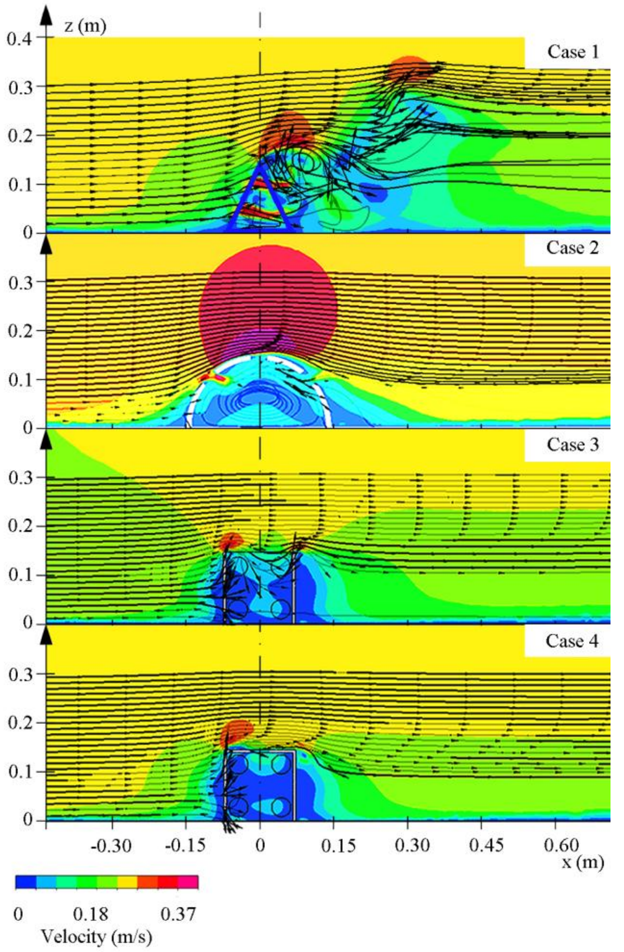

Fig. 7. Flow field of the four cases on the vertical plane.

Shown in Fig. 8 is the horizontal plane of the four case. There are flow-decelerating ranges at both front and back of artificial reef and flow-accelerating ranges at left and right sides. Case 1 has the largest wake flow area and Case 2 has the smallest wake flow area according to Fig. 8. But the influence width of the wake flow in the Case 1 decreases first then increases. The flow-accelerating range at the upfront of the artificial reef in the vertical plane is the upwelling flow area; the flow-decelerating range at the back of artificial reef in both the vertical and horizontal plane is wake flow area. The relative influence areas in the two planes are calculated with a Matlab script, by dividing original influence area with the cross-section artificial reef area. The result shows that the triangular prism (Case 1) has the largest upwelling flow and wake flow among the four cases on both the reference plane, which disagrees with the result of length analysis. The upwelling flow is located directly over the dome shell (Case 2) but a slightly behind the triangular prism (Case 1), which may be the reason for the differences in the two analysis methods. Case 4 has a larger influence effect on the surrounding water than Case 3, which means the cover cap has a positive influence on the flow field.

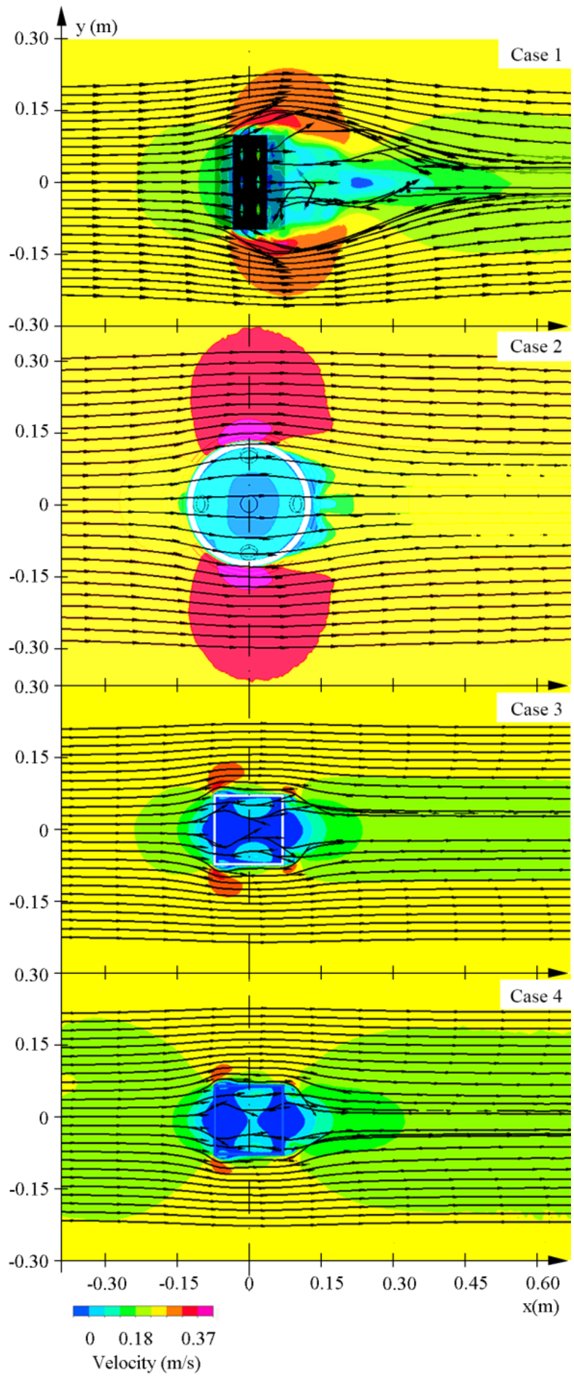

Fig. 8. Flow field of the four cases on the horizontal plane.

C. Influence Volume

The distribution of different velocity value in the calculation domain is presented in Fig. 10. The ordinate axis is the percentage of different velocity volume which is calculated by space integral. Because the velocity of inlet boundary is set as 0.2 m/s, the highest point comes around this value in all the four cases. All the four cases have a large flow-decelerating volume and a small flow-accelerating volume. Case 2 has a relatively smaller flow-decelerating volume and larger flow-accelerating volume compared with other three cases, due to the geometry characters. The flow field changes smoothly and steadily around the streamlined hemispherical shell, which could be seen in the plane analysis above. So the hemispherical shell has a smaller influence effect on the surrounding flow according to the volume analysis.

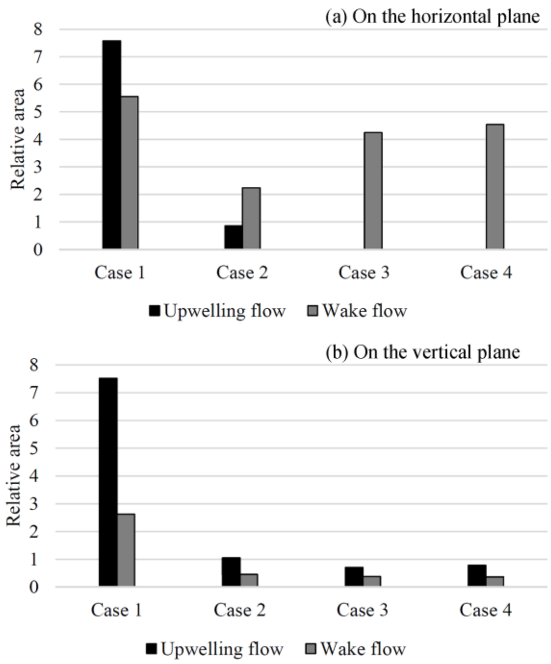

Fig. 9. Relative influence area of the four cases.

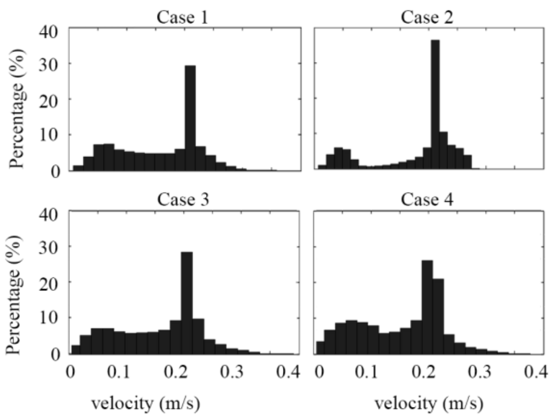

Fig. 10. The distribution of velocity in the calculation domain.

To make the influence zone more distinct and precise, we use a post-CFD program to display the influence zone in Fig. 11. In the Fig. 11 the white part above the artificial reef is the flow-accelerating zone where the velocity is higher than 1.2 times of inlet velocity [15]. The other part with green or yellow color is the flow-decelerating zone where the velocity is less than 0.8 times of inlet velocity. As described in the above section, the flow-decelerating zone which at the back of the artificial reef is wake flow zone, the flow-accelerating zone which at the upfront of the artificial reef is the upwelling flow zone. The back eddy zone is not presented here because of the limitation of the length of this paper. But the volume of back eddy zone, wake flow zone, and upwelling flow zone are shown in Fig. 12. The relative volume in Fig. 12 is calculated by dividing the three kinds of influence volume with the physical volume of artificial reefs. Shown in Fig. 12, the triangular prism (Case 1) has a larger influence volume than any of other three kinds of artificial reefs. Cube shell without a cover cap (Case 3) has a smaller influence volume in general compared with Case 4.

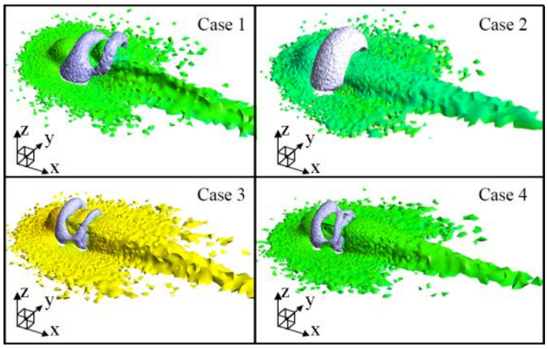

Fig. 11. The influence volume of four cases.

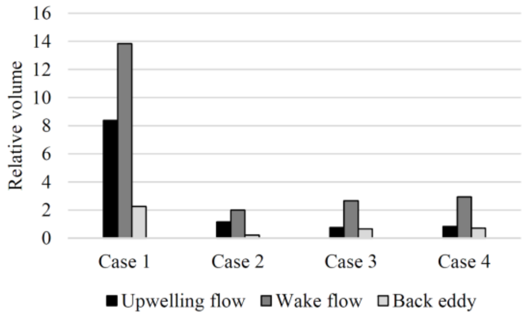

Fig. 12. Relative influence volume of the four cases.

V. Conclusion

In this paper, three measurements are discussed for the physical influence of artificial reefs. According to the results and analysis presented above, the most representative reference value may be the influence volume. The other two methods can also be a good way to indicate the detail of wake flow and upwelling flow but back eddy. All the three measurement methods should be used together to analyze the influence effect with different weights. This paper can be a preparation for the analytic hierarchy process (AHP) for the artificial reef design and optimize.

Acknowledgment

The present research is supported by the Marine Nonprofit Industry-Specific (201305030, 201303047) and National Natural Science Foundation of China (31072246).

References

[1] W. Seaman and M. Miller, "Fishery conservation and habitat improvement in marine ecosystems," *Reconciling Fisheries with Conservation, Vols I and Ii*, vol. 49, pp. 881-889, 2008.
[2] Y. X. Zhang and X. L. Zheng, "Experimental study on fish attractive effects of artificial reef models," *Advances in Environmental Technologies, Pts 1-6*, vol. 726-731, pp. 357-362, 2013.
[3] O. Langhamer, D. Wilhelmsson, and J. Engstrom, "Artificial reef effect and fouling impacts on offshore wave power foundations and buoys - a pilot study," *Estuarine Coastal and Shelf Science*, vol. 82, pp. 426-432, Apr 30 2009.
[4] Y. X. Zheng, Z. L. Liang, C. T. Guan, X. F. Song, J. Li, Y. Cui, Q. Li, and Y. Zhou, "Numerical simulation and experimental study of the effects of disposal space on the flow field around the combined three-tube reefs," *China Ocean Engineering*, vol. 29, pp. 445-458, Jun 2015.
[5] D. Kim, J. Woo, H. S. Yoon, and W. B. Na, "Wake lengths and structural responses of Korean general artificial reefs," *Ocean Engineering*, vol. 92, pp. 83-91, Dec. 1, 2014.

[6] T. L. Liu and D. T. Su, "Numerical analysis of the influence of reef arrangements on artificial reef flow fields," *Ocean Engineering*, vol. 74, pp. 81-89, Dec. 1, 2013.

[7] Z. Y. Jiang, Z. L. Liang, L. Y. Huang, Y. Liu, and Y. L. Tang, "Characteristics from a hydrodynamic model of a trapezoidal artificial reef," *Chinese Journal of Oceanology and Limnology*, vol. 32, pp. 1329-1338, Nov. 2014.

[8] Z. Y. Jiang, Z. L. Liang, Y. Liu, Y. L. Tang, and L. Y. Huang, "Particle image velocimetry and numerical simulations of the hydrodynamic characteristics of an artificial reef," *Chinese Journal of Oceanology and Limnology*, vol. 31, pp. 949-956, Sep. 2013.

[9] V. Yakhot, S. A. Orszag, S. Thangam, T. B. Gatski, and C. G. Speziale, "Development of turbulence models for shear flows by a double expansion technique," *Physics of Fluids a-Fluid Dynamics*, vol. 4, pp. 1510-1520, Jul. 1992.

[10] C. C. Chang and B. S. Lin, "Renormalization group analysis of magnetohydrodynamic turbulence with the Alfven effect", *Journal of the Physical Society of Japan*, vol. 71, pp. 1450-1462, Jun. 2002.

[11] L. M. Smith and S. L. Woodruff, "Renormalization-group analysis of turbulence," *Annual Review of Fluid Mechanics*, vol. 30, pp. 275-310, 1998.

[12] J. C. F. Pereira and J. M. P. Rocha, "Prediction of stably stratified homogeneous shear flows with second-order turbulence models," *Fluid Dynamics Research*, vol. 42, pp. Aug. 2010.

[13] S. S. Lu, C. H. Lee, and H. Ozoe, "Numerical treatment of pressure boundary conditions in SIMPLEC," *Progress in Computational Fluid Dynamics*, vol. 9, pp. 269-276, 2009.

[14] Y. Liu, Y. P. Zhao, G. H. Dong, C. T. Guan, Y. Cui, and T. J. Xu, "A study of the flow field characteristics around star-shaped artificial reefs," *Journal of Fluids and Structures*, vol. 39, pp. 27-40, May. 2013.

[15] D. J. Priour, "Ocular myiasis in a Texas sheep shearer", *Tex Med*, vol. 76, pp. 52-53, Oct. 1980.

Huang Luiyi was born in Huaining in 1970. He received the bachelor degree in fishery engineering, a master degree in fishing science, and a doctoral degree in enrichment and aquaculture engineering from the Ocean University of China in 1993, 2006, and 2013, respectively.

His areas of research interest are theoretical and experimental researches on the hydrodynamic characteristics of fish cages of aquaculture and development of the sea-cage system, the selectivity of fishing gears and development of selective fishing equipments, hydrodynamic properties of net twines, and offshore aquatic-breeding facilities.

Prof. Huang is a member of China Society of Fisheries, China Fisheries Committee for Standardization, and Qingdao Fishery Production Safety Expert Group.

Cheng Hui was born in Qingdao in 1991. He received the bachelor degree in marine fishery science and technology from the Ocean University of China in 2014. He is pursuing his master degree in fishing science from the Ocean University of China now.

His areas of research interest are fishing technology, trawl design and optimizing, fish behavior, artificial reef and ecosystem restoration, hydrodynamic properties of net twines, and coastal engineering.

Mr. Cheng is a volunteer of Greenpeace, Clean Ocean Action, and World Fisheries Trust.

Tang Yanli was born in Liaocheng in 1965. He received the bachelor degree, master degree, and a doctoral degree in marine fishing engineering from the Ocean University of China in 1985, 1992, and 2013, respectively

His areas of research interest are fishing gears and development of ocean-friendly and effective fishing technology, the selectivity of fishing gears and its effect on the eco-friendly fishing method, and artificial fish reef engineering and its effect on the recovery and enrichment of fish resources.

Prof. Tang is a member of the Ministry of Marine Fishing Gear Expert Committee, Shandong Ocean Farm Observational Network, and Qingdao Fishery Production Safety Expert Group.

Yang Qian was born in Meishan in 1992. She received the bachelor degree in marine fishery science and technology from the Ocean University of China in 2014. She is pursuing her master degree in marine life science from the Tokyo University of Marine Science and Technology now.

Her areas of research interest are trawl selectivity and optimizing, fish behavior, and artificial reef ecosystem restoration.

Wang Xinxin was born in Yichun in 1980. She received the bachelor degree in mathematics, a master degree in computational mathematics from the Ocean University of China in 2003 and 2006, respectively.

Her areas of research interest are theoretical, experimental researches and numerical simulations on the hydrodynamic characteristics of the fish cages of aquaculture and development of sea-cage system, hydrodynamics properties of new twines, the fluid characteristics of new twines, the fluid characteristics of the artificial reefs, and the wave responses of the submersible rafts in the deep sea.